

promoting access to White Rose research papers



Universities of Leeds, Sheffield and York
<http://eprints.whiterose.ac.uk/>

This is an author produced version of a paper published in **Nature Climate Change**.

White Rose Research Online URL for this paper:

<http://eprints.whiterose.ac.uk/77975/>

Paper:

Iizumi, T, Sakuma, H, Yokozawa, M, Luo, JJ, Challinor, AJ, Brown, ME, Sakurai, G and Yamagata, T (2013) *Prediction of seasonal climate-induced variations in global food production*. *Nature Climate Change*, 3. 904 - 908.

<http://dx.doi.org/10.1038/nclimate1945>

Prediction of seasonal climate-induced variations in global food production

Toshichika Iizumi ^{1*}, Hirofumi Sakuma ^{2, 3}, Masayuki Yokozawa ¹, Jing-Jia Luo ⁴, Andrew J. Challinor ^{5, 6}, Molly E. Brown ⁷, Gen Sakurai ¹, and Toshio Yamagata ³

¹ National Institute for Agro-Environmental Sciences, Tsukuba, Japan

² Research Institute for Global Change, Yokohama Institute for Earth Sciences, JAMSTEC, Yokohama, Japan

³ Application Laboratory, Yokohama Institute for Earth Sciences, JAMSTEC, Yokohama, Japan

⁴ Centre for Australian Weather and Climate Research, Bureau of Meteorology, Melbourne, Australia

⁵ Institute for Climate and Atmospheric Science, School of Earth and Environment, University of Leeds, Leeds, UK

⁶ CGIAR-ESSP Program on Climate Change, Agriculture and Food Security (CCAFS), Department of Plant and Environmental Sciences, Faculty of Science, University of Copenhagen, Frederiksberg, Denmark

⁷ Biospheric Sciences Branch, NASA Goddard Space Flight Center, Greenbelt, MD, USA

Consumers, including the poor in many countries, are increasingly dependent on food imports¹ and are therefore exposed to variations in yields, production, and export prices in the major food-producing regions of the world. National governments and commercial entities are therefore paying increased attention to the cropping forecasts of major food-exporting countries as well as to their own domestic food production. Given the increased volatility of food markets and the rising incidence of climatic extremes affecting food production, food price spikes may increase in prevalence in future years²⁻⁴. Here we present a global assessment of the reliability of crop failure hindcasts for major crops at two lead times derived by linking ensemble seasonal climatic forecasts with statistical crop models. We found that moderate-to-marked yield loss over a substantial percentage (26–33%) of the harvested area of these crops is reliably predictable if climatic forecasts are near perfect. However, only rice and wheat production are

reliably predictable at three months before the harvest using within-season hindcasts. The reliabilities of estimates varied substantially by crop—rice and wheat yields were the most predictable, followed by soybean and maize. The reasons for variation in the reliability of the estimates included the differences in crop sensitivity to the climate and the technology used by the crop-producing regions. Our findings reveal that the use of seasonal climatic forecasts to predict crop failures will be useful for monitoring global food production and will encourage the adaptation of food systems to climatic extremes.

Although global crop monitoring and yield prediction models (e.g., the Global Information and Early Warning System of the FAO⁵ and the Famine Early Warning Systems Network⁶) have been developed, few studies have evaluated the reliability of seasonal climatic forecast-based cropping predictions on a global scale to date. However, global commodity markets are essential to maintaining national food balances and affordable access for consumers, including the poor^{7,8}. Large increases in food prices since 2008, occurring as a result of the widespread drought in crop-export regions in 2008 and 2012, coupled with a transforming food system (i.e., the increasing production of biofuels) increase the importance of being able to anticipate large changes in food production⁹⁻¹¹. These changes affect both the rural and urban poor who are reliant on imports from the global commodity market to ensure that a sufficient amount of food is available to meet demand.

We conducted a global overview of the reliability of crop failure forecasts for maize, rice, wheat, and soybean, which are the principal cereal and legume crops worldwide, providing nearly 60% of all calories produced on croplands¹². The key question posed was “How reliable is the forecasting of crop failure at lead times that allow such information to be of value to governments and commercial concerns?” Previous work on this topic focused on predicting extreme events with either a smaller geographical focus¹³ or by using methods that limited their usefulness in connection to broader climate modeling efforts¹⁴.

We assessed the reliability of “hindcasts” (i.e., retrospective forecasts for the past) of crop yield loss relative to the previous year for two lead times. Pre-season yield predictions employ climatic forecasts and have lead times of approximately 3 to 5 months for providing information regarding variations in yields for the coming cropping season (Fig. 1). Within-season yield predictions use climatic forecasts with lead times of 1 to 3 months. Pre-season predictions can be of value to national governments and commercial concerns, complemented by subsequent updates from within-season predictions. The latter incorporate information on the most recent climatic data for the upcoming period of reproductive growth¹⁵. In addition to such predictions, hindcasts using the re-analyzed historical climatic data (i.e., observations) were performed to demonstrate the upper limit of the reliability of crop forecasting.

Hindcasts using the re-analyzed climatic data for the 1983-2006 interval indicated that the upper limits of prediction of moderate-to-marked (5% more) yield losses were reliably captured ($R^2 \geq 0.301$ when reported and hindcast yield losses were compared; $P < 0.05$) by modeling from 26-33% of the total crop areas harvested worldwide in 2000 (Fig. 2; Table S1). These areas accounted for 28-40% of the world

crop production in that year. The reliability of the estimates of yield levels (including values that were approximately normal or beyond normal) when using the re-analyzed climatic data was comparable to that of the estimates of crop failures mentioned above (Figs. 2, S1). If such reliability is to be realized for not only crop failures but also yield levels, both temperature and soil moisture forecasts must be near perfect.

When within-season hindcasts were evaluated, good reliability was evident in a number of areas throughout the world, including major crop-producing regions, such as Southeast Asia for rice and Australia for wheat (Fig. 3). With climatic hindcasts, the capability of modeling was more distinct when identifying the occurrences of crop failures than when predicting all of the year-to-year variations in yield levels throughout the years (Figs. 3, S2). Note, however, that reported crop yields are not always reliable over the time series used in this analysis, and the results for some countries should be interpreted with caution.

Comparatively higher reliability of pre-season hindcasts was found in areas with similar within-season hindcasts (e.g., Southeast Asia for rice; Figs. S3, S4), although such reliability gradually decreased with increasing lead time (Table S1), as has been previously reported¹⁶. However, the ability of modeling to capture crop failures (17-21% of total production; Fig. S3; Table S1) was still higher in comparison to that of predicting yield levels (5-11% of total production; Figs. S4; Table S1).

Of the total crop area harvested worldwide, 15-19% accounted for 15% to 23% of world production appeared to be reliable when the within-season crop failure hindcasts were evaluated (Fig. 3; Table S1). This result indicates that the crop failure hindcasts for all crops attained more than 50% of their predictive potential whereas yield hindcasts achieved considerably less than 36% of their potential. For both crop failures and yield levels, the hindcast values for rice and wheat, the production of which appears to be more sensitive to temperature than to soil moisture content (Fig. 4), were better at both lead times than the values obtained from the random hindcasts (the comparisons were significant at the 1% level; Fig. S5). By contrast, the hindcast values for maize and soybean conducted at both lead times (the production of which is more sensitive to soil moisture content than to temperature; Fig. 4) were not significantly better than the random hindcast values (Fig. S5).

The observed spread in hindcast yield reliability across different crop types reflects the finding that temperature hindcasts are far more reliable than predictions of soil moisture content at both lead times (Figs. S6, S7). Higher hindcast temperature reliability plays a certain role with respect to gaining the reliability of within-season cropping hindcasts in irrigated cropland, which covers approximately 20% of cultivated land and accounts for over 40% of world production¹⁷, although more land is rainfed area (Fig. S8). This tendency is particularly true in irrigated areas where yields are sensitive to temperature, likely because temperature is a major driver of yield variations if a crop is irrigated sufficiently, whereas the soil moisture content is still important under insufficient irrigation conditions, as suggested by a previous study¹⁸.

Additionally, the hindcast climatic reliability was higher when data from low latitudes were evaluated rather than those from the mid-to-high latitudes (Figs. S6, S7); this conclusion is similar to that obtained in earlier studies¹⁹. Of the top four countries in terms of maize and soybean production (the USA, Brazil, China, and Argentina), all but Brazil are located at mid-latitudes, whereas rice is widely produced (particularly in the tropics) and wheat is grown more extensively worldwide than any other crop (Fig. S9;

Table S1). For wheat in particular, the timing of the growing season is important: a large proportion of wheat is grown in winter. Winter climate forecasts in the northern hemisphere are typically more accurate than summer forecasts because the extratropical winter atmosphere is strongly influenced by events in tropical regions and because the effects of tropical climatic variations on winter climatic patterns in the northern hemisphere are stronger than on that of the summer²⁰. Because of differences in the characteristics of production systems, the reliability of the estimates of rice and wheat yield losses was highest, distantly followed by those of soybean and maize (Fig. S5; Table S1). For the estimates of yield levels, wheat prediction was most reliable, followed by the estimates of rice, soybean, and maize (Table S1).

The relatively high reliability of hindcasts to capture the crop failures of rice and wheat and to predict the year-to-year variations in wheat yield levels in particular encouraged us to extract further information. The areas for which within-season hindcasts of yield levels are available include four of the major wheat-exporting countries, namely, the USA, France, Canada, and Australia. Together, these regions produced 53% of the world wheat export in 2008 (Fig. S10). In these areas, within-season hindcasts were reliable for 9% to 35% of the harvested area (Fig. 5), suggesting that up to 11% of all wheat exports from these four countries are predictable (27% of world wheat exports were predictable when the data from all wheat-exporting countries were considered; Table S1). When the pre-season yield hindcasts were evaluated, the area for which the predictions were reliable was lower (1-32% of all harvested areas in the exporting countries mentioned above; Fig. 5); however, the reliability level was similar to that afforded by the analysis of within-season hindcasts from the USA and Australia.

In contrast, the levels of rice exports that were reliably predicted were far lower than those of wheat exports when the yield hindcasts were evaluated but were comparable when the crop failure hindcasts were assessed (Table S1). Notably, a considerable extent of the predictable area (52-78% of the national harvested area) found in the third-major rice exporter, Uruguay, contributed to results in such values for predicting the rice yield losses (Fig. S11). The second-major rice exporter, Thailand, exhibited even less predictable area (3% of the national harvested area); although Thailand is located in the tropics, this result is likely due to the lack of crop calendar data for the triple cropping systems under operation in that region^{21, 22} and the higher sensitivity of yields to soil moisture conditions (Fig. 4).

We found that the principal features of climate-induced crop failures in a substantial percentage of the global crop-growing regions were reliably predictable for rice and wheat but were less predictable for maize and soybean. The particular features of global production systems allow reliable estimates of crop failure, including a notable association between crop yields and ambient temperature, an extensive growth area worldwide (or within the tropics), significant production from winter cropping, and accurate estimates of winter temperatures. Notably, the areas within which the occurrences of crop failures (or yield levels) are reliably predictable include the countries that are major exporters of wheat and rice. This finding suggests that modeling can potentially yield information on the seasonal climate-induced variability in the production levels of rice and wheat in major exporter countries and that such estimates can be made available 3 to 5 months before harvest. Such information would be of value to both national governments and commercial entities for maintaining an adequate

national food balance and ensuring adequate responses to major food crises. These data, when combined with satellite-derived information on rainfall levels and the extent of vegetative productivity²³, can support a range of decisions, including the adaptation of food systems for the poor to climatic extremes and, ultimately, to climate change.

However, considerable work is required to produce operational forecasts because yield levels do not exclusively determine the extent to which food is supplied to commodity markets and prices. Sociopolitical factors (i.e., the Russian wheat embargo of 2010–2011²⁴) often critically influence the world food supply and are often motivated by crop failures induced by climatic extremes. Decision makers struggle to respond within a timely manner if predictions remain uncertain for even a few months of lead²⁵.

The predictions derived from the modeling presented here or from more plant physiological process-based crop models of this type^{16, 26, 27} can be used to establish a global crop failure prediction system. Although process-based models may be promising at specific sites¹⁶, there is a lack of global historical crop datasets, which would be required for more sophisticated representations of hybrid seeds, planting dates, and nitrogen, water, and chemical inputs. Furthermore, the methods of climate impact assessment have tended to use yield variability as a measure of uncertainty, instead of assessing changes in crop yield variability²⁸. We demonstrate the potential for skilful predictions of crop failures, which in turn suggest that the limitation of qualitative methods can be addressed. In demonstrating the potential value of quantitative prediction methods, this study also supports evidence²⁹ for the potential use of such methods in regions where qualitative methods currently dominate, for example, sub-Saharan Africa¹³.

METHODOLOGICAL SUMMARY

Climate and crop data for the 1982–2006 interval were collected by using a grid with a resolution of 1.125° in both latitude and longitude. The temperature and soil moisture data were downloaded from the JRA-25 monthly re-analyzed dataset³⁰. For each of the four crops, all re-analyzed data were averaged over the reproductive growth periods, as determined from the global crop calendar dataset²¹. Thus, the climatic features specific to individual locations, over the months of crop growth, were considered.

Nine ensemble seasonal climatic hindcasts (three physically perturbed models, for which three sets each of initial conditions were used) were generated by using the SINTEX-F ocean/atmosphere-coupled general circulation model; the prediction lead

times ranged from 1 to 12 months²⁰. The lead data for 1 to 3 and 3 to 5 months were averaged to yield the within-season and pre-season hindcasts, respectively. Biases in the global climate model predictions for temperature and soil moisture were removed before analysis.

Crop yields were obtained from the global historical yield dataset²², which aligns the FAO yield data and grid yield proxy information derived from satellite-derived net primary productivity.

The crop and climate data were combined as follows: (1) a first-difference time series was computed by using the yield levels and a re-analysis of the temperature and soil moisture data. (2) Each first-difference yield was divided by the 3-year average of the yield to derive the percentage first-difference values. (3) A multiple linear regression model was constructed for each cropping system. (4) Weighted-average yields were calculated by using the production levels by cropping system as weighting factors. (5) Regression coefficients were determined on a year-by-year basis by using the leave-one-out cross-validation method. Finally, (6) all bias-corrected climatic forecasts were subjected to regression modeling to derive the hindcast data (the percentage changes in yield from that of the previous year).

1. Food and Agriculture Organization of the United Nations (FAO). *The State of Food Insecurity in the World: How does international price volatility affect domestic economies and food security?* (FAO, 2011).
2. Funk, C. C. & Brown, M. E. Declining global per capita agricultural production and warming oceans threaten food security. *Food Sec.* **1**, 271–289 (2009).
3. FAO. *Report of the FAO Expert Meeting on How to Feed the World in 2050* (FAO, 2009).
4. Intergovernmental Panel on Climate Change (IPCC). *Managing the Risks of Extreme Events and Disasters to Advance Climate Change Adaptation* (Cambridge University Press, 2012).
5. FAO, *Global Information and Early Warning System on Food and Agriculture* <http://www.fao.org/gIEWS/english/index.htm> (2012).
6. Famine Early Warning System Network, *Famine Early Warning System Network* <http://www.fews.net/Pages/default.aspx> (2012).

7. Ravallion, M., Chen, S., & Sangraula, P. *New evidence on the urbanization of global poverty* (World Bank, 2007).
8. Ruel, M. T., Garrett, J. L., Hawkes, C., & Cohen, M. J. The food, fuel, and financial crises affect the urban and rural poor disproportionately: A review of the evidence. *J. Nutr.* **140**, 170S-176S (2010).
9. Rosegrant, M. W., Msangi, S., Sulser, T. & Valmonte-Santos, R. *Biofuels and the Global Food Balance. 2020 Vision for Food, Agriculture and the Environment* (International Food Policy Research Institute, 2006).
10. Headey, D. & Fan, S. Anatomy of a crisis: the causes and consequences of surging food prices. *Agric. Econ.* **39**, 375–391 (2008).
11. Stringer, L. C. et al. Adaptations to climate change, drought and desertification: local insights to enhance policy in southern Africa. *Environ. Sci. and Policy* **12**, 748–765 (2009).
12. Ray, D. K., Ramankutty, N., Mueller, N. D., West, P. C., Foley, J. A. Recent patterns of crop yield growth and stagnation. *Nat. Commun.* **3**, 1293 (2012).
13. Hansen, J. W., Mason, S. J., Sun, L. & Tall, A. Review of seasonal climate forecasting for agriculture in sub-Saharan Africa. *Exp. Agric.* **47**, 205-240 (2011).
14. Lenton, T. M. What early warning systems are there for environmental shocks? *Environ. Sci. & Policy* **24**, S60-S75 (2012).
15. Cane, M. A., Eshel, G., & Buckland, R. W. Forecasting Zimbabwean maize yield using eastern equatorial Pacific sea surface temperature. *Nature* **370**, 204-205 (1994).
16. Hansen, J. W., Challinor, A. J., Ines, A. V. M., Wheeler, T. R., & Moron, V. Translating climate forecasts into agricultural terms: advances and challenges. *Clim. Res.* **33**, 27-41 (2006).
17. World Water Assessment Programme (WWAP). *The United Nations World Water Development Report 4: Managing Water under Uncertainty and Risk* (United Nations Educational, Scientific and Cultural Organization, 2012).
18. Hawkins, E. et al. Increasing influence of heat stress on French maize yields from the 1960s to the 2030s. *Glob Change Biol.* **19**, 937-947 (2013).
19. Wilks, D. S., & Godfrey, C. M. Diagnostic verification of the IRI net assessment forecasts, 1997–2000. *J. Clim.* **15**, 1369–1377 (2002).

20. Luo, J.-J., Masson, S., Behera, S., Shingu, S., & Yamagata, T. Seasonal climate predictability in a coupled OAGCM using a different approach for ensemble forecasts. *J. Clim.* **18**, 4474-4497 (2005).
21. Sacks, W. J. Deryng, D., Foley, J. A., & Ramankutty, N. Crop planting dates: An analysis of global patterns. *Global Ecol. Biogeogr.* **19**, 607-620 (2010).
22. Iizumi, T. *et al.* Historical changes in global yields: Major cereal and legume crops from 1982 to 2006. *Global Ecol. Biogeogr.* (in review).
23. Funk, C. New satellite observations and rainfall forecasts help provide earlier warning of drought in Africa. *Earth Observer.* **21**, 23-27 (2009).
24. Welton, G. *The Impact of Russia's 2010 Grain Export Ban*, *Oxfam Research Reports*
<http://www.oxfam.org/sites/www.oxfam.org/files/rr-impact-russias-grain-export-ban-280611-en.pdf> (2011).
25. Vogel, C., & O'Brien, K. Who can eat information? Examining the effectiveness of seasonal climate forecasts and regional climate-risk management strategies. *Clim. Res.* **33**, 111-122 (2006).
26. Challinor A.J., Ewert, F., Arnold, S., Simelton, E., & Fraser, E. Crops and climate change: progress, trends, and challenges in simulating impacts and informing adaptation, *J. Exp. Bot.* **60**, 2775-2789 (2009).
27. Iizumi, T., Yokozawa, M., & Nishimori, M. Parameter estimation and uncertainty analysis of a large-scale crop model for paddy rice: Application of a Bayesian approach. *Agric. For. Meteorol.* **149**, 333-348 (2009).
28. Easterling, W. E. *et al.* in *Climate Change 2007: Impacts, Adaptation and Vulnerability* (eds. Parry, M. L. *et al.*) (Cambridge University Press, 2007).
29. Vermeulen, S. J. *et al.* Addressing uncertainty in adaptation planning for agriculture. *Proc. Nat. Acad. Sci. USA* (in press).
30. Onogi, K. *et al.* The JRA-25 Reanalysis. *J. Meteorol. Soc. Japan* **85**, 369-432 (2007).

Supplementary Information. Supplementary information is included in the online version of the present publication.

Correspondence and requests for materials should be addressed to T.I. (e-mail: iizumit@affrc.go.jp)

Acknowledgements. We thank R.C. Stone, P. McIntosh, H. Kanamaru, and M. Otsuka for helpful comments on the earlier version of this manuscript. T.I. was supported by the Japan Society for the Promotion of Science (JSPS) Grant-in-Aid for Research Activity Start-up (23880030). T.I, M.Y., and G.S. were supported by the Environment Research and Technology Development Fund (S-10-2) of the Ministry of the Environment, Japan. The Science and Innovation Section of the British Embassy in Tokyo provided us with the opportunity to conduct this study via a UK–Japan workshop arrangement.

Author Contributions. T.I. was responsible for the study design, data analysis, and manuscript preparation. J.J.L. contributed seasonal climatic forecasting and assisted in manuscript preparation. G.S. provided the computational code used to optimize the crop yield modeling. H.S., M.Y., A.J.C., M.E.B, and T.Y. assisted with the study design and helped write the manuscript.

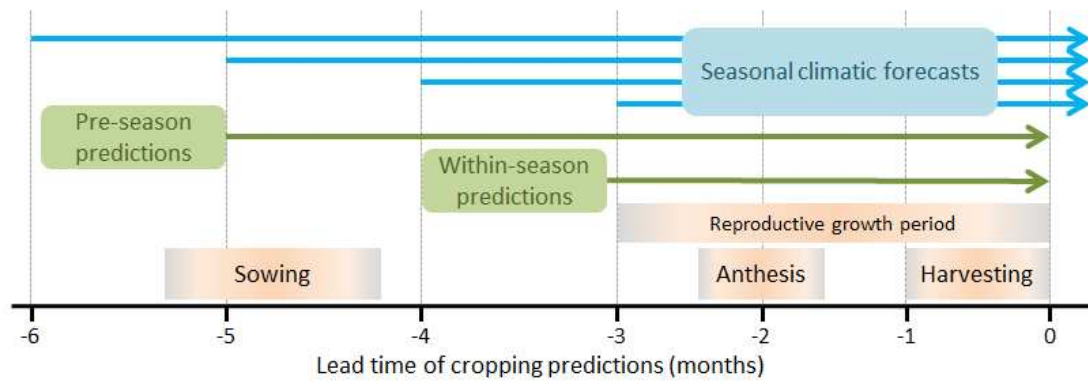


Figure 1. Timing of cropping predictions. The cropping calendar illustrates the times at which the pre- and within-season predictions of crop failures and yield levels were conducted and the lead times of seasonal climatic forecasts on a monthly basis.

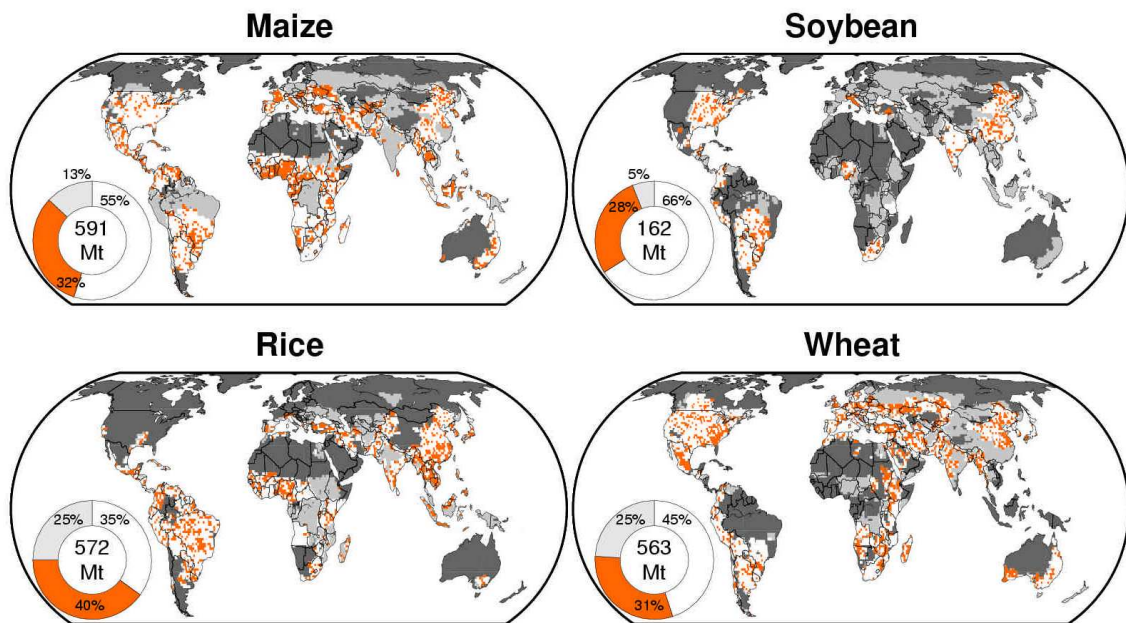


Figure 2. The upper limits of reliability when moderate-to-marked yield losses of maize, soybean, rice, and wheat were hindcasted via re-analysis data. White—the yield losses were less reliably estimated (the coefficients of determination, R^2 , between the reported and hindcast yields over the 1983–2006 period <0.454 , $n=10$, $P>0.05$). Orange—the yield losses could be reliably estimated ($R^2 \geq 0.454$, $n=10$, $P<0.05$). Light gray—no hindcast were produced because the crop calendar is lacking. Dark gray—non-cropland. The pie diagrams indicate the percentages of production from the areas. All data in the pie diagrams are normalized against the world production in 2000.

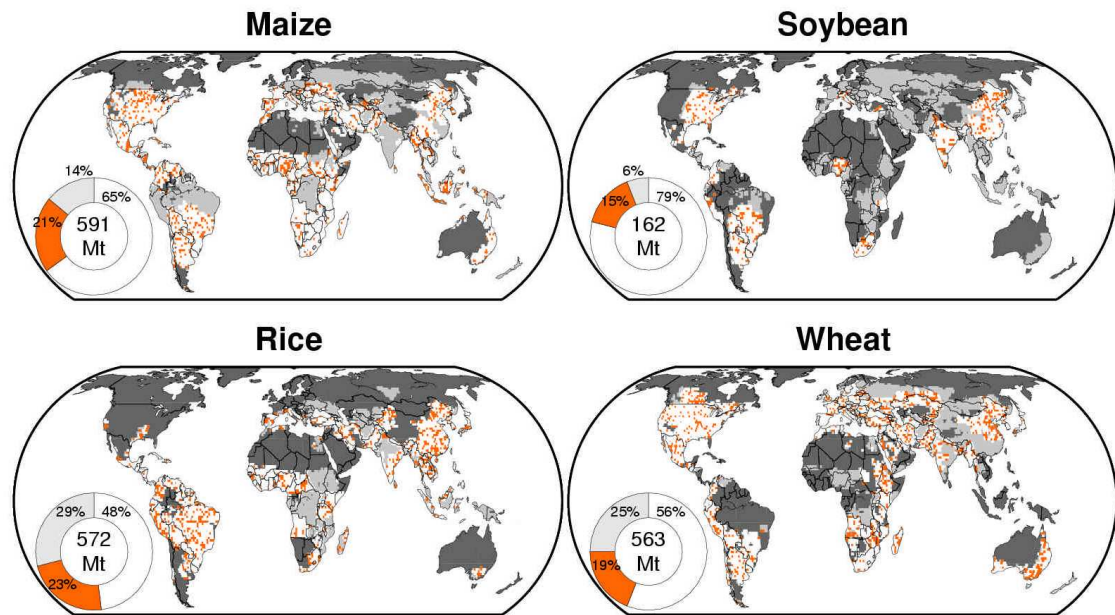


Figure 3. The reliability of the within-season hindcasts of the moderate-to-marked (5% more) yield losses for maize, soybean, rice, and wheat. The legend for Figure 2 is also applicable to this figure, although the within-season (and not the pre-season) hindcasts were derived. $R^2 < 0.301$ and $R^2 \geq 0.301$ (both, $n=10$, $P < 0.05$) were used for the areas in white and orange, respectively.

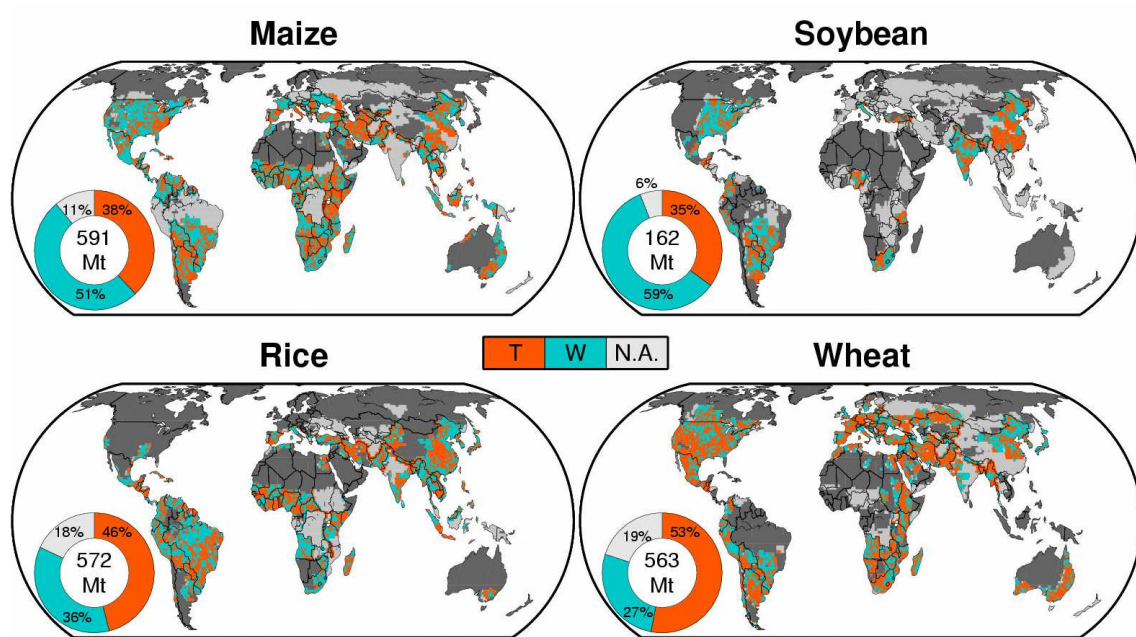


Figure 4. The dominant climatic factors affecting the year-to-year variations in the yields of maize, soybean, rice, and wheat. The pie diagrams indicate the percentages of production that are sensitive to temperature (red) and soil moisture content (blue) as well as those for which no hindcasts were available (gray) in 2000. The dark gray area indicates non-cropland.

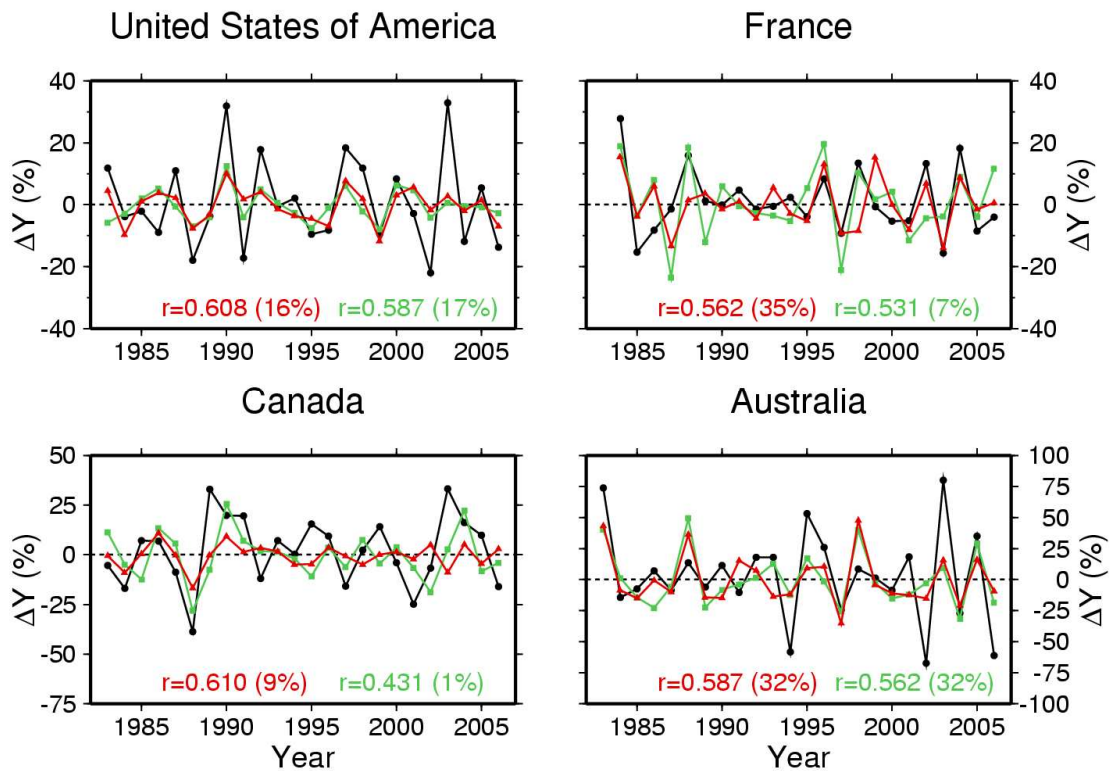


Figure 5. The capture reliability of the year-to-year relative wheat yield variations for the reliable areas in four major wheat-exporting countries (the USA, France, Canada, and Australia). The reported yields (black), pre-season hindcasts (green), and within-season hindcasts (red) are presented. The “*r*” values are correlation coefficients, which were calculated by comparing the reported values with that obtained from the two hindcasts. All correlations were significant at the 5% level. The numbers in parentheses are the percentages of areas for which yields were reliably predictable among all of the harvested areas within each country.

Prediction of seasonal climate-induced variations in global food production

SUPPLEMENTARY METHODS

Climate data

The monthly historical temperature and soil moisture data from regions gridded at a scale of 1.125° in both latitude and longitude were obtained from the Japanese re-analysis (called JRA-25) dataset³⁰. The re-analyzed soil moisture was estimated from a multi-layer thermo-dynamical land surface model that considers the precipitation, evaporation, vegetation respiration, soil water holding capacity, run-off, and other processes. On a monthly mean basis, the temporal variation patterns of the data accurately matched *in situ* soil moisture observations collected in Illinois, USA³⁰. For each cropping system of a crop of interest, the data from each cell were temporally averaged over the reproductive growth period. We considered the reproductive growth period to be a 3-month interval, commencing 3 months before harvesting and ending at harvesting; this interval completely covered each key growth period (Fig. 1). For each cropping system, the month of harvest in each grid cell was determined by using the global crop calendar dataset²¹. A dataset containing information on the global harvested areas³¹ was used to identify the grid cells in which a crop of interest was grown.

Nine-member monthly temperature and soil moisture forecasts were generated using the SINTEX-F ocean/atmosphere-coupled general circulation model (GCM)²⁰. The ensemble featured three initial conditions for each of the three physically perturbed models, thereby accounting for the uncertainties in both the model physics and initial conditions. The initial conditions were generated by assimilating only the observed sea surface temperature data into the coupled model and by considering three different restoring times for temperature in a 50-m surface mixed layer^{20, 32}. This approach is effective for generating operational seasonal climatic forecasts. Ensemble mean values were calculated for each forecast at various lead times, ranging from one to 12 months. Next, the forecast data averaged over the reproductive growth period of each cropping system of a crop of interest were computed in a manner similar to that employed in re-analysis. Pre- and within-season hindcasts were constructed based on the lead data

for 3 to 5 and 1 to 3 months; these hindcasts roughly correspond to the so-called “seasonal climate outlook” and “seasonal weather forecasts”¹³, respectively. The GCM biases in temperature and soil moisture relative to the re-analysis (but not the prediction errors in these climatic variables) were removed by using a cumulative distribution function-based correction method³³. Such bias correction rendered the 25-year (1982–2006) mean forecast values the same as those obtained upon re-analysis, although temporal variations in the forecast patterns were not affected by such corrections.

Crop yield data

Yearly crop yield data from areas gridded at a scale of 1.125° in both latitude and longitude were obtained from a newly developed global gridded dataset that contains information on historical crop yields²². The dataset aligns the FAO country yield statistics with grid yield estimates based on the net primary production values derived from the Advanced Very High Resolution Radiometer of the National Ocean and Atmosphere Administration (NOAA/AVHRR). The grid yield estimates were validated by comparison with independent subnational yield data from the major producing countries²² and a global dataset of crop yields in 2000³⁴. However, the yield data are not always reliable over the analyzed period, and the results for some countries (in particular, Africa and South Asia) should be interpreted with caution because the reported yields from countries in these regions are often estimated with reference solely to the local weather conditions. This dataset contained information on the yields of multiple cropping systems for maize, rice, and wheat and that of a single cropping system for soybean. However, only aggregated data on the yields from various cropping systems were available when the present analysis was conducted.

Statistical crop models

Yearly time series of cropping and climatic data were combined as follows to derive multiple linear regression models. For a crop of interest, a first-difference time series was initially computed to provide the yield:

$$\Delta Y_{t,g} = \frac{(Y_{t,g} - Y_{t-1,g})}{Y_{t-3t-1,g}} \times 100, \text{ (Eq. S1)}$$

where the suffixes t and g indicate the year and grid cell, respectively. $\Delta Y_{t,g}$ is the first-difference yield percentage in year t (%); $Y_{t,g}$ and $Y_{t-1,g}$ indicate the yields in year t and in the previous year ($t-1$) ($t \text{ ha}^{-1}$); and $\bar{Y}_{t-3:t-1,g}$ is the average yield for the interval from year $t-3$ to year $t-1$ ($t \text{ ha}^{-1}$). Calculation of the first-difference yields emphasizes the change in yield due to short-term, primarily climate-related factors, although demand, prices, technological improvements, and other factors affect the year-to-year variations in both yields and production. The same average yield was used for each of the first 4 years of analysis.

Similarly, first-difference time series were computed using the mean re-analysis temperature ($\Delta T_{t,g}$, °C) during the reproductive growth period and the soil water content for the first soil layer from the ground surface to a 10-cm depth ($\Delta S_{t,g}$, mm):

$$\Delta T_{t,g} = T_{t,g} - T_{t-1,g}, \text{ (Eq. S2)}$$

$$\Delta S_{t,g} = S_{t,g} - S_{t-1,g}. \text{ (Eq. S3)}$$

We used the 10-cm soil moisture data after confirming that the use of moisture data from different soil depths yielded similar results. Although the reproductive growth period-mean soil moisture was negatively correlated with the mean temperature for the same period to some extent, it was still more strongly correlated with the mean precipitation for that period than the temperature in many regions (Fig. S12).

Although the vegetative growth period is important in terms of crop growth, yields are more sensitive to climatic conditions during the reproductive growth period (particularly around the time of anthesis) than to those at any other growth period^{35, 36}. Thus, statistical crop modeling frequently employs climatic variables averaged over the reproductive growth period, or over a specific phenological stage, as informative variables³⁷.

Next, a multiple linear regression model was computed for each cropping system of a crop of interest:

$$\Delta Y_{t,g,c} = \alpha_{g,c} \cdot \Delta T_{t,g,c} + \beta_{g,c} \cdot \Delta S_{t,g,c} + \gamma_{g,c} + \varepsilon, \text{ (Eq. S4)}$$

$$\Delta Y_{t,g} = \frac{\sum_{c=1}^C w_{g,c} \cdot \Delta Y_{t,g,c}}{\sum_{c=1}^C w_{g,c}}, \text{ (Eq. S5)}$$

where the suffixes t , g , and c denote year, grid cell, and cropping system of a crop of interest, respectively. $\Delta Y_{t,g,c}$ is the percentage first-difference in yield when cropping

system c of a crop of interest is used (%); $\Delta T_{t,g,c}$ and $\Delta S_{t,g,c}$ are the first-difference values of the re-analysis mean temperature ($^{\circ}\text{C}$) and the soil moisture value (mm) during the reproductive growth period; $\alpha_{g,c}$, $\beta_{g,c}$, and $\gamma_{g,c}$ are regression coefficients; ε is the error term; $w_{g,c}$ is the production level of a crop of interest using cropping system c (tonnes); and C is the number of cropping systems employed to produce each crop of interest. Two cropping system types (major/second or winter/spring) were used to produce the models of maize, rice, and wheat, whereas a single cropping system was employed to produce the soybean model. The production levels yielded by the application of various cropping systems in different countries during the 1990s were obtained from the U.S. Department of Agriculture³⁸.

The regression coefficients were determined in a probabilistic manner by using the Markov Chain Monte Carlo (MCMC) method²⁷. The prior distribution setup was non-informative in nature, which made it possible to use the MCMC approach to explore possible uncertainties in the values of the regression coefficients as widely as possible. The convergence of such values to posterior distributions was analyzed using the approach of Gelman and Rubin³⁹. A single set of regression coefficients associated with the highest likelihood values was used to assess the crop yield hindcast reliability at two lead times, whereas the posterior probability distributions of such coefficients were used to measure the uncertainties associated with the likelihood values when the hindcasts obtained by using statistical cropping models were compared with the data generated by using random hindcasts (please see the section on “**Random yield hindcasting**” for details).

We used the leave-one-out cross-validation method to evaluate the current crop yield prediction and its reliability. For each grid cell, we removed one of 24 samples (i.e., the first-difference yield time series over the 25 years evaluated) and estimated the parameter values under such conditions. Next, the statistical crop model was used to predict the value of the sample removed from the calibration data; a single set of parameter values affording the highest likelihood was used in such calculations. This exercise was repeated with the sequential individual removal of all 24 samples.

The bias-corrected mean temperature and soil moisture forecasts during the reproductive growth period of each crop of interest grown by using different cropping systems, as calculated at two lead times, were incorporated into the regression models

calibrated using the re-analysis climatic data to predict the year-to-year variations in relative yield.

Random yield hindcasting

To measure the reliability of hindcasts of 5% more yield losses, we generated random cropping hindcasts and compared these predictions with the test values. For any given grid cell and crop type, we first pooled the percentage first-difference time series values of the reported yields ($\Delta Y_{t,g}$, $t = 1983 \dots 2006$) and the randomly sampled $\Delta Y_{t,g}$ values for the 24-year period in which data were available; identical values were accepted. Second, we calculated the determination coefficients (R^2) values between the reported and generated $\Delta Y_{t,g}$ time-series values (only the reported 5% more yield losses and the sampled values in the corresponding years were considered in the analysis); the extent of reliable production was determined next (please see the “**Definition of predictive reliability**” section for details). Finally, such random sampling was iterated 10,000-fold to obtain a probability density distribution (PDF) of the reliability of the production loss levels derived using random hindcasting.

We next calculated the uncertainty levels of crop hindcasting by comparing the reliable production loss levels obtained when random and seasonal climatic prediction-based crop hindcasting steps (the latter is termed “model hindcasting”) were performed. Each PDF of the reliable production loss values obtained by using model hindcasting was calculated as follows. First, for a given grid cell and cropping system of a crop of interest, we sampled the regression coefficients from the posterior distributions determined by using the MCMC method; then, we calculated the $\Delta Y_{t,g}$ time series over the study period. Only the single-ensemble mean temperature and soil moisture forecast were used as inputs because such forecasts are generally more accurate than any other single-ensemble forecast. Second, the R^2 values were obtained by comparing the real $\Delta Y_{t,g}$ time series with that obtained by model hindcasting (only the reported 5% more yield losses and hindcast values in the corresponding years were used); the extent of the reliable production loss level was then calculated. Finally, such sampling was iterated 10,000-fold.

To compare the random and model hindcasts for each crop, we obtained a

measure of the reliable production prediction, Q_{random} , from random hindcasting and a similar measure, Q_{model} , from model hindcasting, by using data from the PDFs. Next, Q_{model} was compared with Q_{random} to explore whether the null hypothesis, $Q_{random} \geq Q_{model}$, was or was not rejected. Finally, we iterated such sampling 100,000-fold and calculated the proportion of instances (relative to the total number of iterations) in which the null hypothesis was rejected, yielding the p -values. The mean production loss levels that could be reliably predicted, and the associated 95% probability intervals, obtained by using the random and model hindcasts were calculated at two lead times with reference to the PDF values associated with the reliable predictions of production loss.

Determination of the dominant climatic factors

The dominant climatic factor (i.e., either the mean temperature or soil moisture content over the reproductive growth period) was determined by comparing the extent of (percentage) change in the year-to-year relative yield with the unit changes in temperature and soil moisture content *via* data re-analysis:

$$\frac{\partial \Delta Y_{g,c}}{\partial \Delta T_{g,c}} = \alpha_{g,c} \frac{\overline{\Delta T_{g,c}}}{\overline{\Delta Y_{g,c}}} \text{ and } \frac{\partial \Delta Y_{g,c}}{\partial \Delta S_{g,c}} = \beta_{g,c} \frac{\overline{\Delta S_{g,c}}}{\overline{\Delta Y_{g,c}}} \text{ (Eq. S6)}$$

$$\frac{\partial \Delta Y_g}{\partial \Delta T_g} = \frac{\sum_{c=1}^C w_{g,c} \frac{\partial \Delta Y_{g,c}}{\partial \Delta T_{g,c}}}{\sum_{c=1}^C w_{g,c}} \text{ and } \frac{\partial \Delta Y_g}{\partial \Delta S_g} = \frac{\sum_{c=1}^C w_{g,c} \frac{\partial \Delta Y_{g,c}}{\partial \Delta S_{g,c}}}{\sum_{c=1}^C w_{g,c}}, \text{ (Eq. S7)}$$

where the suffixes g and c denote the grid cell and cropping system used for production of the crop of interest, respectively. $\partial \Delta Y_{g,c} / \partial \Delta T_{g,c}$ and $\partial \Delta Y_{g,c} / \partial \Delta S_{g,c}$ reflect the influence of the (percentage) changes in mean temperature and soil moisture content over the reproductive growth period, respectively, on the (percentage) changes in the year-to-year relative yield variation when cropping system c was used. $\overline{\alpha}_{g,c}$ and $\overline{\beta}_{g,c}$ are the most likely values of the regression coefficients for $\alpha_{g,c}$ and $\beta_{g,c}$, respectively, derived using the MCMC method. $\overline{\Delta Y}_{g,c}$ is the long-term mean variation in the relative yield. $\partial \Delta Y_{g,c} / \partial \Delta T_{g,c}$ and $\partial \Delta Y_{g,c} / \partial \Delta S_{g,c}$ reflect the influence of the (percentage) changes in mean temperature and soil moisture content, respectively, on the (percentage) changes in the yield variation of a crop of interest. $w_{g,c}$ is the production level (tonnes) of a crop of interest grown by using cropping system c . We

confirmed that $\overline{\Delta Y}_{g,c}$ had a non-zero value for all grid cells.

The dominant climatic factor for a given grid cell (DCF_g ; a dimensionless parameter) was the factor affecting the yield variation to a greater extent than any other factor. The dominant climatic factor was obtained by comparing the absolute changes in the year-to-year relative yield variations with the unit changes in temperature and soil moisture content:

$$DCF_g \equiv \max\left(\left|\frac{\partial \Delta Y_g}{\partial \Delta T_g}\right|, \left|\frac{\partial \Delta Y_g}{\partial \Delta S_g}\right|\right). \text{ (Eq. S8)}$$

Definition of predictive reliability

For each climatic variable (temperature and soil moisture content) and each lead time (pre- and within-season), the climatic hindcast reliability was measured by calculating the R^2 values using the mean re-analysis data from the reproductive growth period and hindcast values. Therefore, the reliability values that we obtained reflect a correspondence between the yearly temporal variation patterns, as revealed by both the data re-analysis and hindcast. R^2 values greater than 0.163 were deemed “reliable” because such values indicate statistically significant correspondences between re-analysis and hindcasts at the 5% level (measured with the one-tailed t -test) when the sample size (n) was 24 (i.e., using the yearly first-difference time series from the 25-year interval). Use of a one-tailed test is reasonable in the present context; predictive reliability was associated with only positive correlative values.

The reliabilities of crop yield hindcasts for two lead times were also measured by calculating the R^2 values upon comparison of the relative year-to-year variations in the reported and hindcast yields. R^2 values greater than 0.163 indicate “reliable” yield hindcasts ($n=24$). To measure the yield hindcast reliability when using the re-analysis data, determination coefficients adjusted for the degrees of freedom, $Adj-R^2$, were used instead of R^2 values. When the sample size was 24 and there were two explanatory variables (temperature and soil moisture content), $Adj-R^2$ values greater than 0.177 were statistically significant at the 5% level; thus, we deemed such values “reliable” when predicting yield levels using the re-analysis climatic data.

R^2 values greater than 0.301 were used to define “reliable” for the reliability of hindcasts of 5% more yield losses (based on the typical sample size, $n=10$). The

corresponding $Adj-R^2$ values were 0.454. The arrangements of the R^2 and $Adj-R^2$ values were performed to account for the impacts of the sample size and number of explanatory variables on the statistical significance.

Extrapolation to production and exports

The extent of all harvested areas for which predictions were “reliable”, and the levels of production (or production loss) from such grid cells (termed “reliable area” and “reliable production (loss),” respectively) were calculated as follows. First, data on the grid cells for which the R^2 values were greater than 0.163 (for yield hindcasts using climatic hindcasts, but $Adj-R^2$ values of 0.177 for yield hindcasts using the re-analyzed data) were extracted; second, the extent of the harvested areas located within such cells and the crop yields in 2000 were obtained using a global dataset of harvested areas and crop yields³¹; third, for such cells, the harvested areas were multiplied by the yield percentages, and the figures were added to obtain the total production values from the reliable areas; and fourth, the reliable production values were divided by the total world production values in 2000 (calculated by using the global dataset mentioned above³¹). The production percentages that were sensitive to the mean temperature and soil moisture levels over the reproductive growth period were calculated in a similar manner. Additionally, the values for the hindcasts of 5% more yield losses were calculated using R^2 and $Adj-R^2$ values of 0.301 and 0.454, respectively.

The food export amounts from the areas in which the production (loss) levels could be reliably predicted were calculated for each of several countries by multiplying the percentages of the exports by the total production levels in the countries in 2008. The FAO database⁴⁰ was used to calculate the grid export levels in the reliable areas in food-exporting countries. Although the harvested area and yield level data used in the analysis for the year 2000 may have differences if compared to those in the present, global historical harvested area data are lacking.

A comparison of the predictive reliability between irrigated and rainfed croplands

To survey the potential impacts of irrigation on the reliability of cropping prediction, the

global map of monthly irrigated and rainfed crop area in 2000⁴¹ was used. Using the data, we calculated the percentage of area irrigated (and rainfed) that was located within a 1.125° grid cell for each crop of interest. The mean extent of the irrigated (and rainfed) area was calculated by averaging the monthly data over the entire growth period of a crop of interest, as obtained from the global crop calendar dataset²¹. The arranged cells in which the crop was grown were sorted in ascending order, and each top 10% of the irrigated and rainfed areas was categorized as an “irrigated area” or “rainfed area,” respectively. We only used the top 10% samples to avoid cells in which the irrigated and rainfed areas are mixed.

We collected the R^2 values calculated between the reported yield losses and within-season hindcasts over the corresponding cells for each of the four areas, including temperature-sensitive and rainfed (T-R), temperature-sensitive and irrigated (T-I), soil moisture-sensitive and rainfed (S-R), and soil moisture-sensitive and irrigated (S-I). Such data were derived from Figs. 3, 4. Then, a box plot was provided for each area to highlight the differences in the R^2 values as a result of the dominant climatic factor and the agro-ecosystem (irrigated or rainfed).

REFERENCES

31. Monfreda, C., Ramankutty, N., & Foley, J. A. Farming the planet: 2. Geographic distribution of crop areas, yields, physiological types, and net primary production in the year 2000. *Global Biogeochem. Cycles* **22**, GB1022, doi:10.1029/2007GB002947 (2008).
32. Luo, J.-J., Zhang, R., Behera, S., Masumoto, Y., Jin, F.-F., Lukas, R., & Yamagata, T. Interaction between El Nino and extreme Indian Ocean Dipole. *J. Clim.* **23**, 726-742 (2010).
33. Iizumi, T. et al. Evaluation and intercomparison of downscaled daily precipitation indices over Japan in present-day climate: Strengths and weaknesses of dynamical and bias correction-type statistical downscaling methods. *J. Geophys. Res.* **116**, D01111, doi:10.1029/2010JD014513 (2011).
34. You, L., S. Wood, & Wood-Sichra, U. Generating global crop maps: from census to grid. Selected paper, IAAE (International Association of Agricultural Economists)

- Annual Conference, Gold Coast, Australia (2006), Available at: http://www.itpgrfa.net/International/sites/default/files/generating_global_crop.pdf (accessed on 15 February 2013).
35. Wheeler, T. R. et al. The duration and rate of grain growth, and harvest index, of wheat (*Triticum aestivum* L.) in response to temperature and CO₂. *J. Exp. Bot.* **47**, 623-630 (1996).
 36. Nakagawa, H., Horie, T., & Matsui, T. Effects of climate change on rice production and adaptive technologies. In: Mew, T.W., Brar, D.S., Peng, S., Dawe, D., & Hardy, B. (eds) *Rice Science: Innovations and Impact for Livelihood*. IRRI and Chinese Academy of Engineering and Chinese Academy of Agricultural Sciences, 635-658 (2003).
 37. Lobell, D.B. & Field, C.B. Global scale climate-crop yield relationships and the impacts of recent warming. *Environ. Res. Lett.* **2**, 014002 (2007).
 38. United States Department of Agriculture (USDA). *Major world crop areas and climatic profiles* (USDA, 1994).
 39. Gelman, A., & Rubin, D.B. Inference from iterative simulation using multiple sequences. *Stat. Sci.* **7**, 457-511 (1992).
 40. FAO. *FAOSTAT* <http://faostat.fao.org> (2012).
 41. Portmann, F. T., Siebert, S. & Döll, P. MIRCA2000—Global monthly irrigated and rainfed crop areas around the year 2000: A new high-resolution data set for agricultural and hydrological modeling. *Global Biogeochem. Cycles*, **24**, GB1011, doi:10.1029/2008GB003435 (2010).

Table S1. Summary of globally harvested areas and production levels of various crops in 2000; global export levels of the crops in 2008; percentages of cropped areas for which 5% more yield losses were reliably predictable; the production loss levels; the export loss levels; the percentages of cropped areas for which the yield levels were reliably predictable; the production levels; and the export levels, as indicated by the upper limits of the hindcast values (calculated via data re-analysis). Both pre- and within-season hindcasts were used in these calculations. ha: hectare. t: tonnes.

Crop	Global			Reliably predictable by crop failure hindcasts			Reliably predictable by yield hindcasts		
	Harvested area (10 ⁶ ha)	Production (10 ⁶ t)	Export (10 ⁶ t)	Harvested area (%)	Production loss (%)	Export loss (%)	Harvested area (%)	Production (%)	Export (%)
<i>Re-analysis</i>									
Maize	136	591	25	30	32	35	36	36	38
Soybean	74	162	54	26	28	30	33	32	26
Rice	150	572	24	33	40	46	38	45	59
Wheat	209	563	39	30	31	41	48	47	49
<i>Pre-season hindcast</i>									
Maize				17	21	23	7	6	3
Soybean				17	17	17	11	5	3
Rice				17	19	26	8	7	11
Wheat				18	19	16	12	11	24
<i>Within-season hindcast</i>									
Maize				18	21	22	9	8	7
Soybean				15	15	14	8	10	7
Rice				19	23	22	12	11	5
Wheat				18	19	16	14	17	27

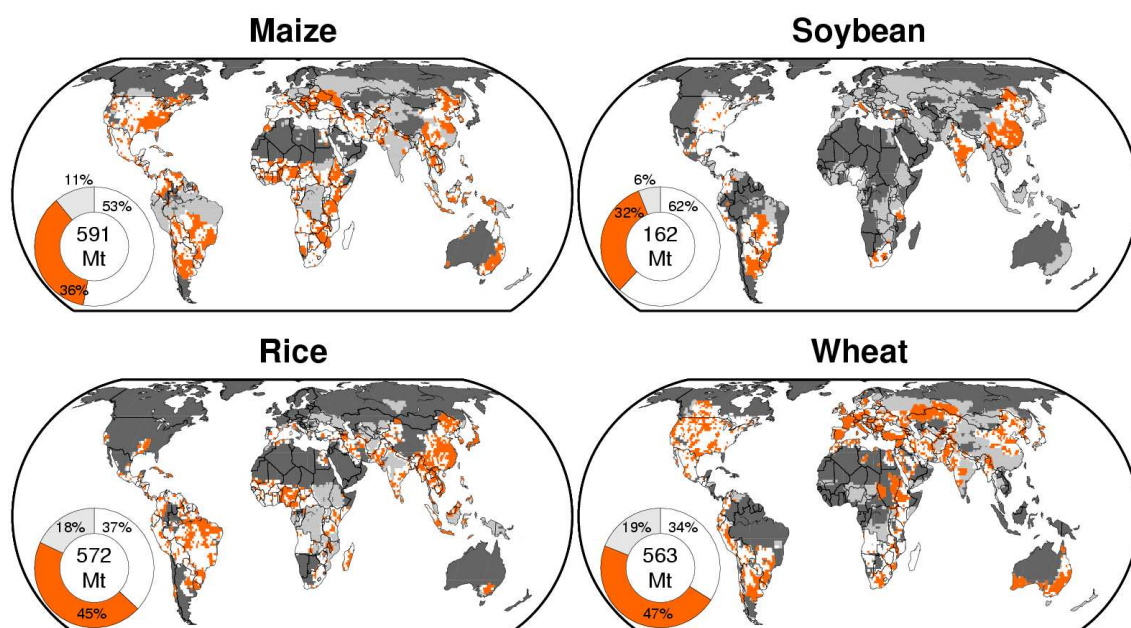


Fig. S1. Upper limits of reliability when the yield levels of maize, soybean, rice, and wheat were hindcasted *via* re-analysis data. White—yields were less reliably estimated (the coefficients of determination, R^2 , between the reported and hindcast yields over the 1983–2006 <0.177 , $n=24$, $P>0.05$). Orange—yields could be reliably estimated ($R^2 \geq 0.177$, $n=24$, $P<0.05$). Light gray—no hindcast was possible because the crop calendar is lacking. Dark gray—non-cropland. Pie diagrams indicate the percentages of production sourced from the above areas. All data in the pie diagrams are normalized against the world production levels in 2000.

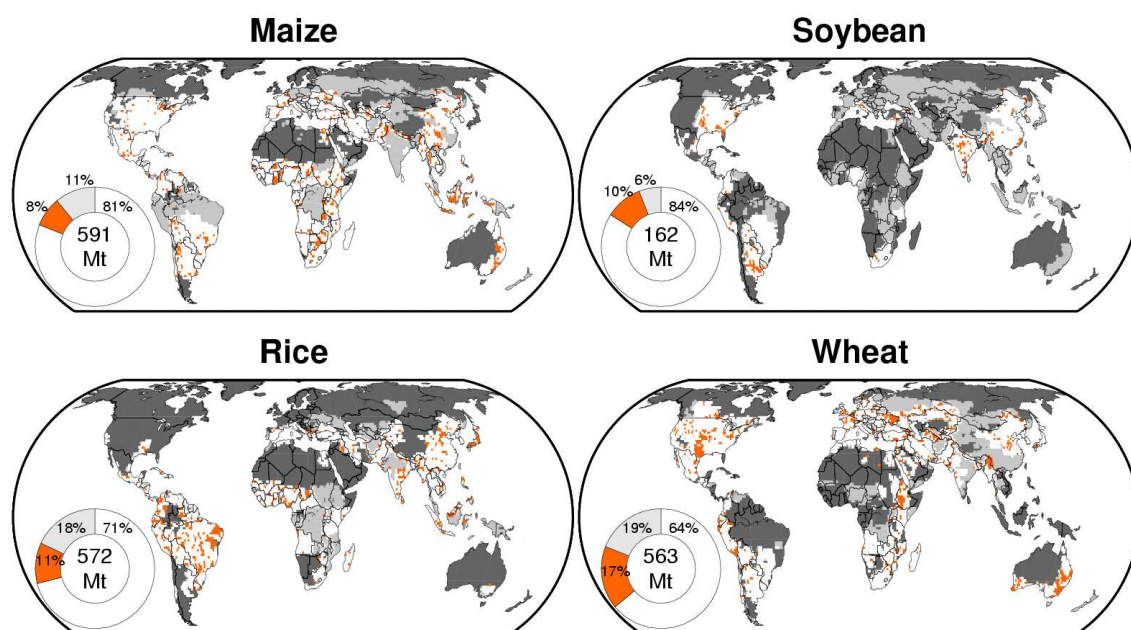


Fig. S2. Reliability of the within-season yield hindcasts for maize, soybean, rice, and wheat. Legend of Fig. S1 is applicable to this figure, except that the within-season (not the pre-season) hindcasts were derived. $R^2 < 0.163$ and $R^2 \geq 0.163$ (both, $n=24$, $P < 0.05$) were used for the areas in white and orange, respectively.

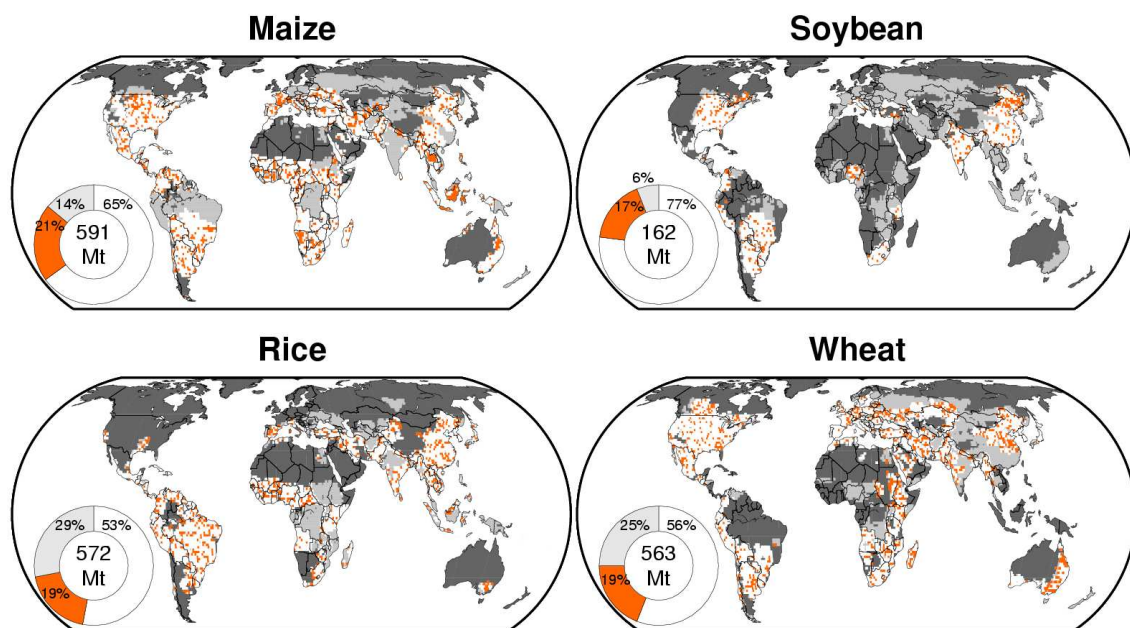


Fig. S3. Reliability of the pre-season hindcasts of the moderate-to-marked yield losses for maize, soybean, rice, and wheat. White—yield losses were less reliably estimated (the coefficients of determination, R^2 , between the reported and hindcast yields over the 1983–2006 <0.301 , $n=10$, $P>0.05$). Orange—yield losses could be reliably estimated ($R^2 \geq 0.301$, $n=10$, $P<0.05$). Light gray—no hindcast was obtained because the crop calendar is lacking. Dark gray—non-cropland. Pie diagrams indicate the percentages of production sourced from the above areas. All data in the pie diagrams are normalized against the world production levels in 2000.

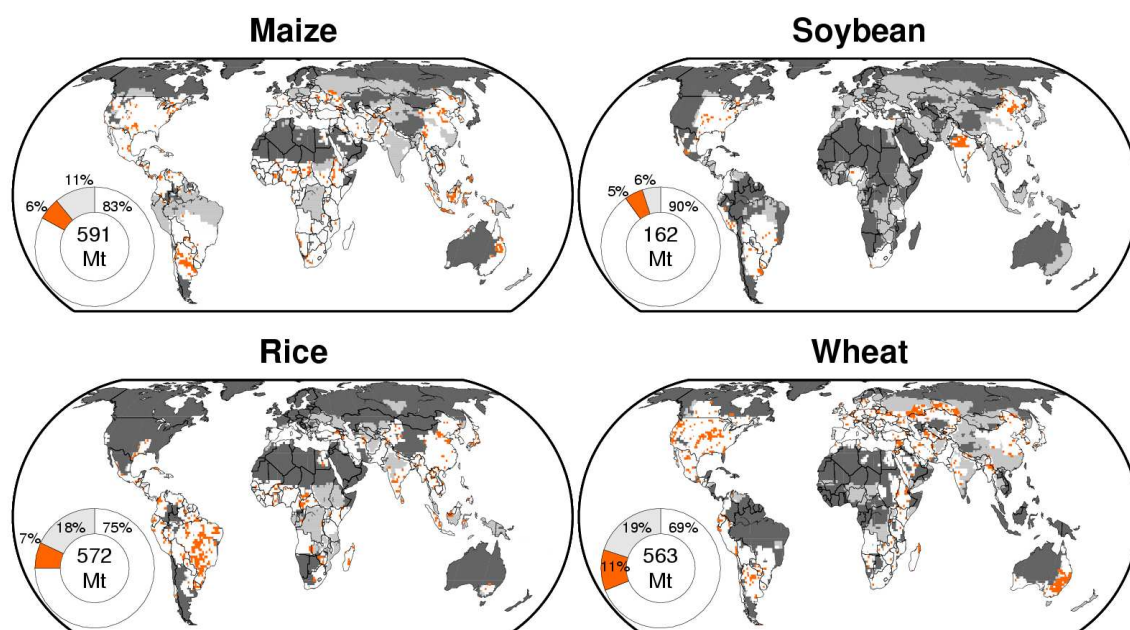


Fig. S4. Reliability of the pre-season yield hindcasts for maize, soybean, rice, and wheat. Legend of Fig. S2 is applicable to this figure, except that the pre-season (not the within-season) hindcasts were derived. $R^2 < 0.163$ and $R^2 \geq 0.163$ (both, $n=24$, $P < 0.05$) were used for the areas in white and orange, respectively.

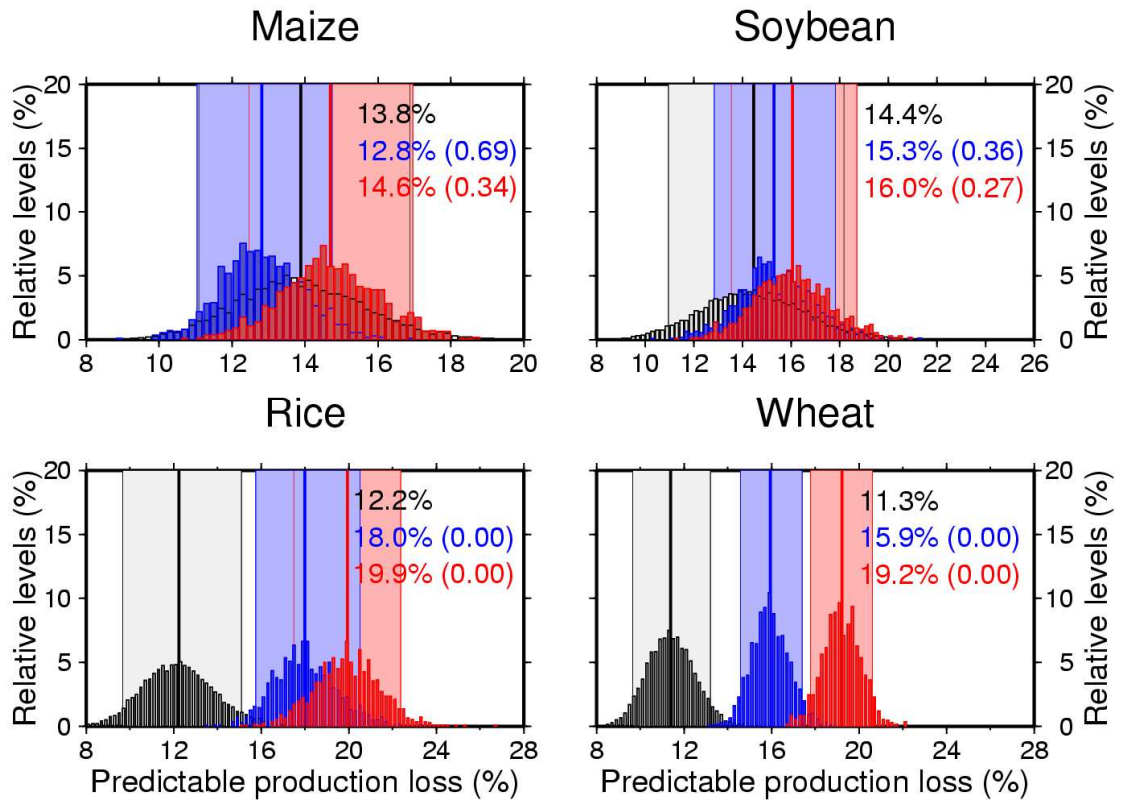


Fig. S5. Probabilities that the levels of production loss were reliably predicted when the random hindcasts and pre- and within-season hindcasts were conducted. Empirical probability density functions (PDFs) of the crop production loss for the areas in which such production loss was reliably predictable by the pre-season hindcasts (blue), within-season hindcasts (red), and random hindcasts (black) are shown. Each PDF was calculated by using a single ensemble of the mean temperature and soil moisture hindcasts and the perturbed crop model parameter values (within the posterior distributions). Colored shading and vertical lines indicate, respectively, the 95% confidence intervals and the means of each hindcast probability. Numbers in each panel are the mean values of reliable production loss estimates with the corresponding p -values in parentheses.

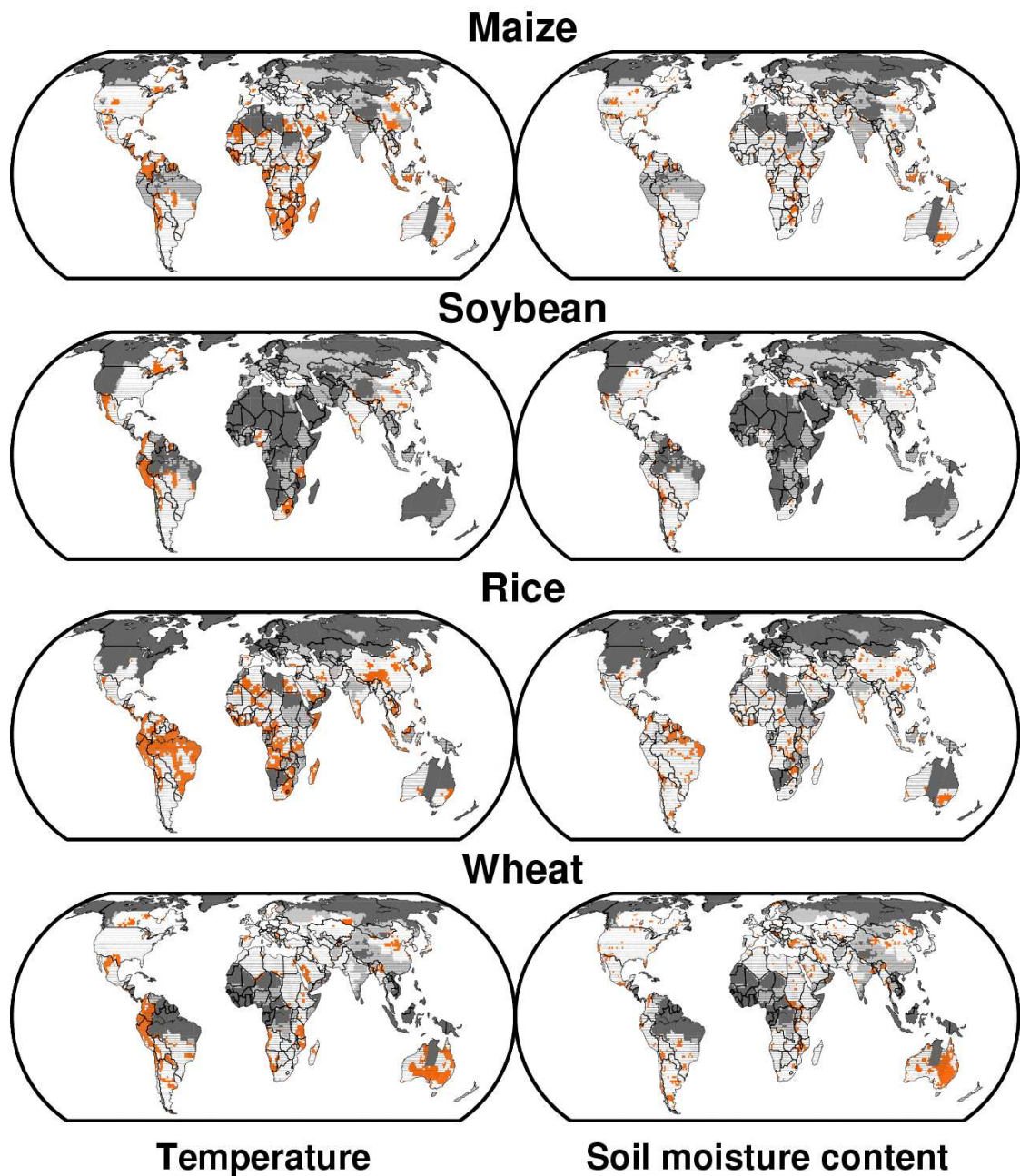


Fig. S6. Determination coefficients (R^2) obtained when the re-analyzed data and the within-season hindcast year-to-year relative temperature and soil moisture variations, obtained over the 1983–2006 period, were compared. Data for maize, soybean, rice, and wheat are shown. White—climatic hindcast was less reliable ($R^2 < 0.163$, $n=24$, $P > 0.05$). Orange—climatic hindcast was reliable ($R^2 \geq 0.163$, $P < 0.05$). Light gray—no hindcast was achieved because the crop calendar is lacking. Dark gray—non-cropland.

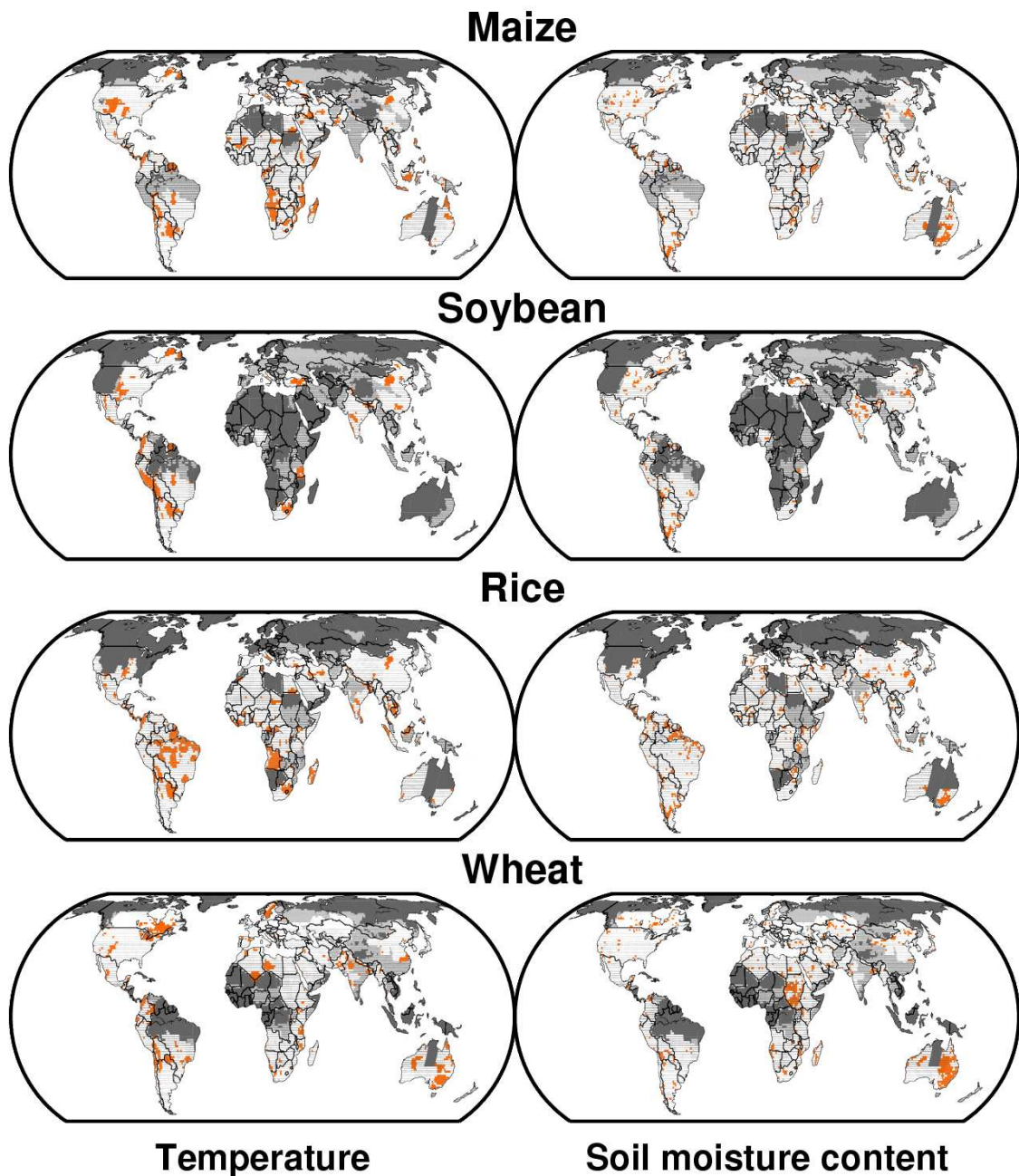


Fig. S7. Determination coefficients (R^2) obtained when the re-analyzed data and the pre-season hindcast year-to-year relative temperature and soil moisture variations, obtained over the 1983–2006 period, were compared. Data for maize, soybean, rice, and wheat are shown. White—the climatic hindcast was less reliable ($R^2 < 0.163$, $n=24$, $P > 0.05$). Orange—the climatic hindcast was reliable ($R^2 \geq 0.163$, $n=24$, $P < 0.05$). Light gray—no hindcast was achieved because the crop calendar is lacking. Dark gray—non-cropland.

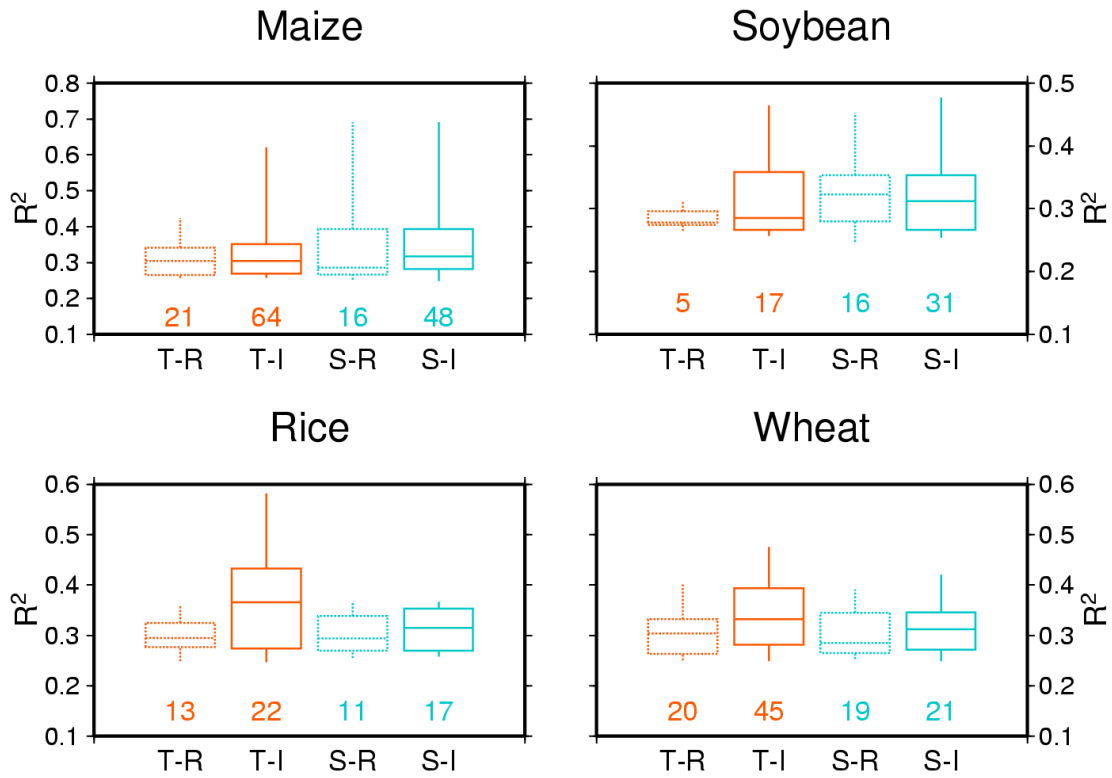


Fig. S8. Box plots of the determination coefficient (R^2) values calculated between the reported and within-season hindcasts of the moderate-to-marked (5% more) yield losses for the four areas: T-R, the temperature-sensitive and rainfed cropland (orange, dashed); T-I, the temperature-sensitive and irrigated cropland (orange solid); S-R, the soil moisture-sensitive and rainfed cropland (blue, dashed); and S-I, the soil moisture-sensitive and irrigated cropland (blue, solid). Horizontal line—median. Lower and upper hinges of a box—the 25% and 50% tiles, respectively. Vertical bar—the 90% interval. Numbers located below each box plot indicate the number of grid cells used in the analysis.

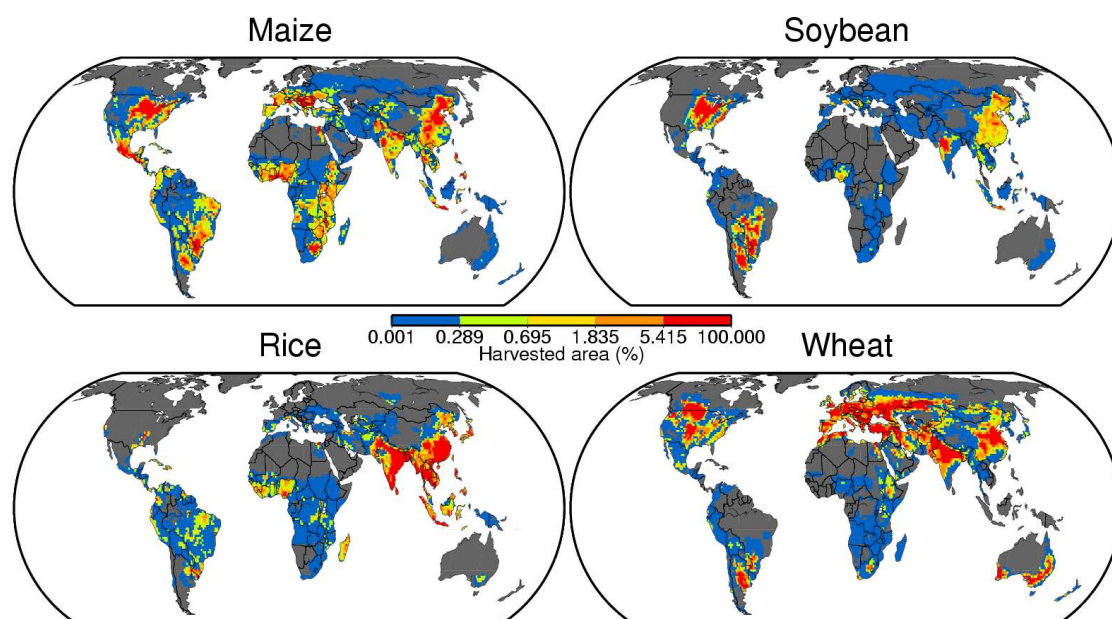


Fig. S9. Geographical distributions, in 2000, of the areas harvested for maize, soybean, rice, and wheat. Coloring indicates the percentages of harvested areas located within a grid cell measuring 1.125° in arc (of both latitude and longitude).

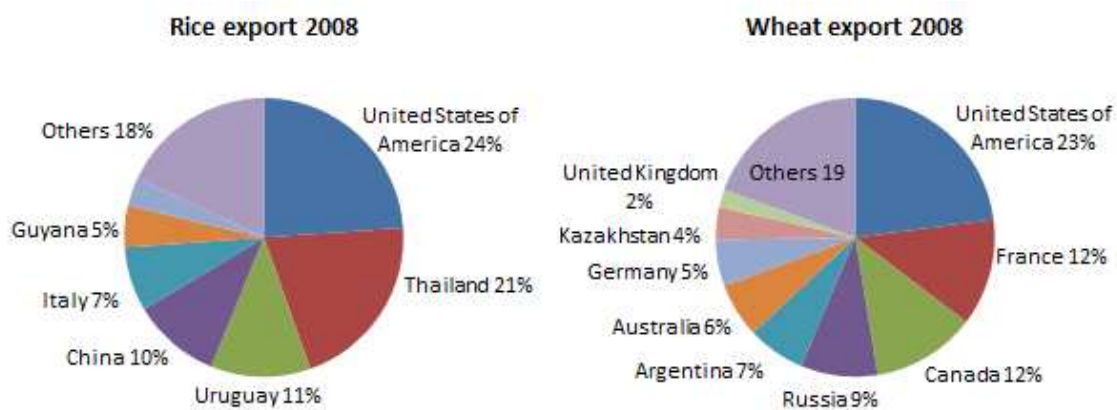


Fig. S10. Global shares of rice and wheat exports, in 2008, by country of production.

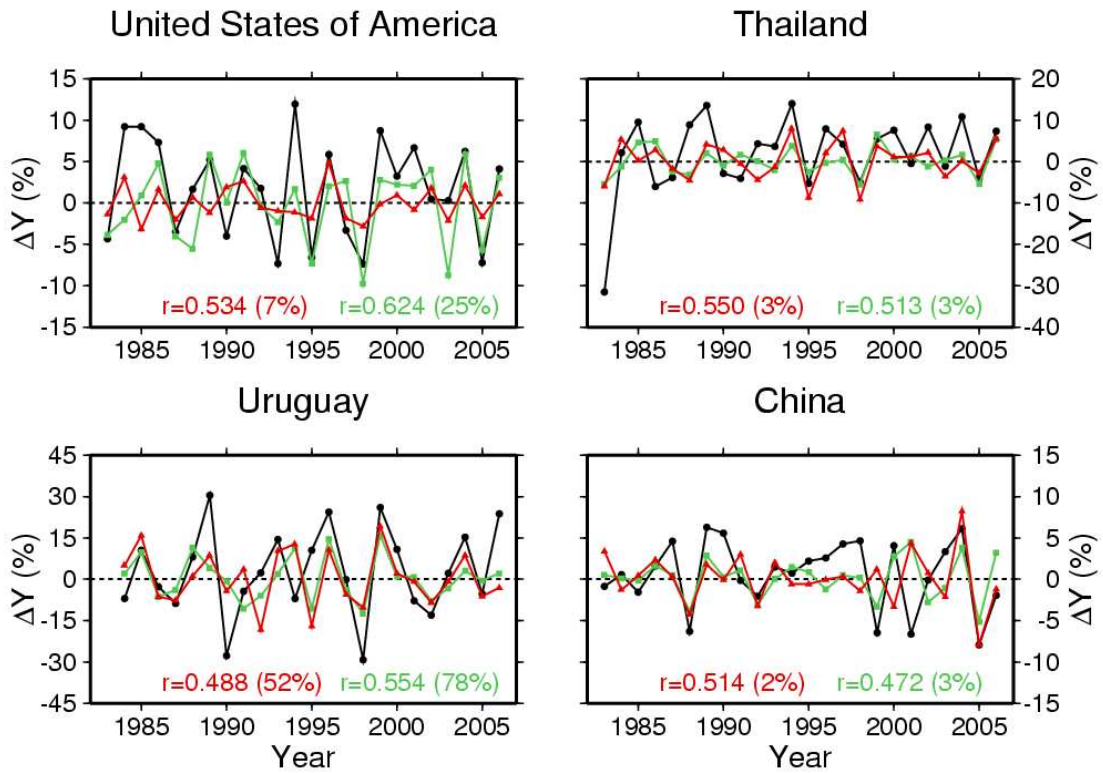


Fig. S11. Capture reliability of the year-to-year relative rice yield variations for reliable areas in four major rice-exporting countries (the USA, Thailand, Uruguay, and China). The reported yields (black), pre-season hindcasts (green), and within-season hindcasts (red) are presented. The “ r ” values are the correlation coefficients calculated by comparing the reported values with the values from each of two hindcasts. All correlations were significant at the 5% level. Numbers in parentheses are the percentages of areas for which the yields were reliably predictable among all harvested areas within each country.

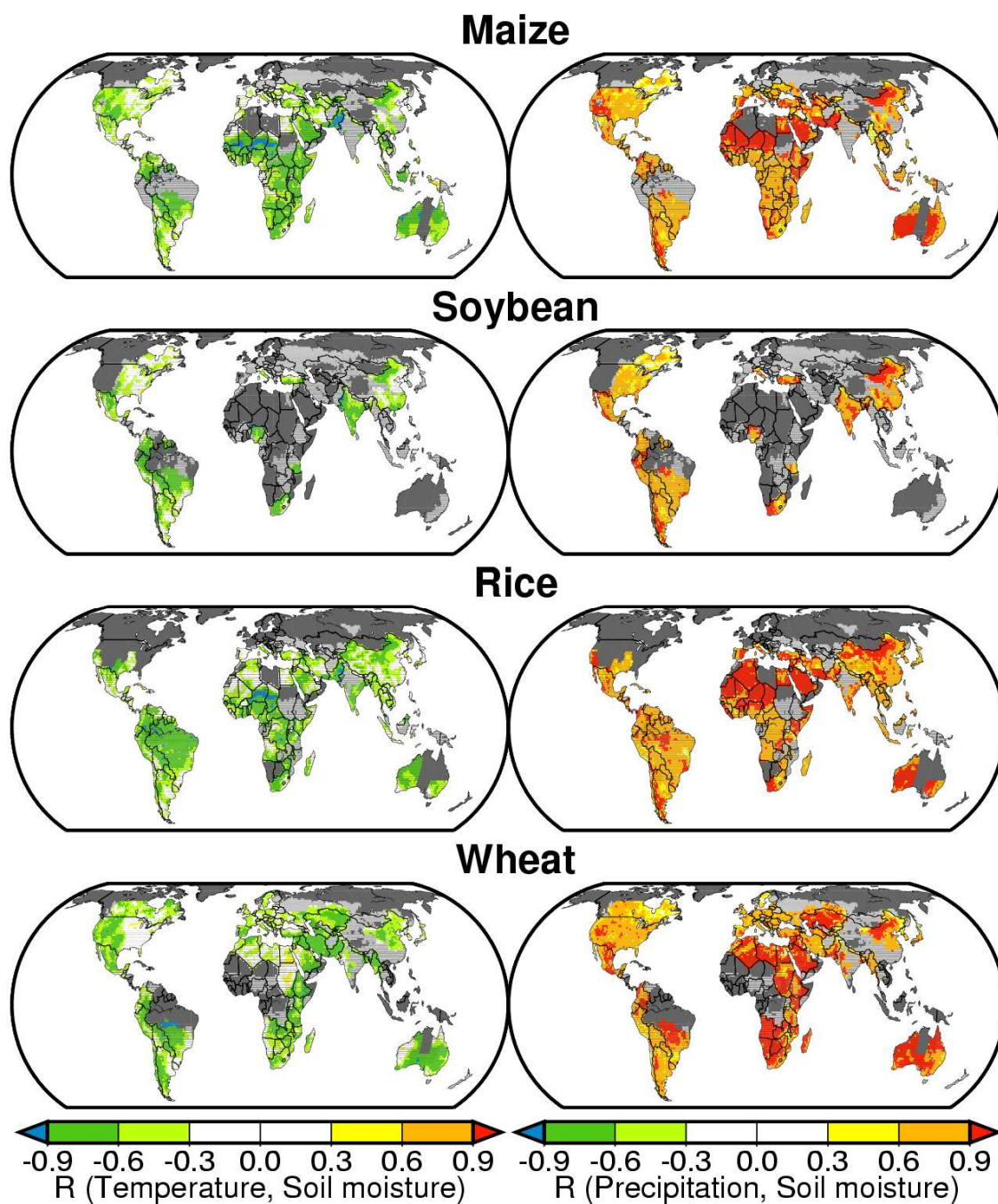


Fig. S12. Correlation coefficients (R) obtained when the reproductive growth period-mean re-analyzed soil moisture, temperature, and precipitation data, obtained over the 1983–2006 period, were compared. Data for maize, soybean, rice, and wheat are shown. Light gray—no hindcast was achieved because the crop calendar is lacking. Dark gray—non-cropland.